

Analytical Methods

Accepted Manuscript



This is an *Accepted Manuscript*, which has been through the Royal Society of Chemistry peer review process and has been accepted for publication.

Accepted Manuscripts are published online shortly after acceptance, before technical editing, formatting and proof reading. Using this free service, authors can make their results available to the community, in citable form, before we publish the edited article. We will replace this *Accepted Manuscript* with the edited and formatted *Advance Article* as soon as it is available.

You can find more information about *Accepted Manuscripts* in the [Information for Authors](#).

Please note that technical editing may introduce minor changes to the text and/or graphics, which may alter content. The journal's standard [Terms & Conditions](#) and the [Ethical guidelines](#) still apply. In no event shall the Royal Society of Chemistry be held responsible for any errors or omissions in this *Accepted Manuscript* or any consequences arising from the use of any information it contains.



Journal Name

ARTICLE

A Free-standing Molecularly Imprinted Photonic Hydrogels Based on β -Cyclodextrin for Visual Detection of L-Tryptophan

Zhaokun Yang, Dongjian Shi, Mingqing Chen, and Shirong Liu*

Received 00th January 20xx,
Accepted 00th January 20xx

DOI: 10.1039/x0xx00000x

www.rsc.org/

Inverse opals of molecularly imprinted photonic hydrogels (CD-MIPHS) based on β -cyclodextrin were firstly elaborated by using the colloidal crystal template method. The film can be exfoliated from the substrate in H_2O to get a free-standing photonic crystal film. L-Tryptophan imprinted polyacrylamide photonic hydrogels (PAM-MIPHS) and CD-MIPHS were fabricated in this paper. The PAM-MIPHS exhibited good sensing property to L-Trp and the redshift of the Bragg diffraction peak was 83 nm. Furthermore, the recognition to L-Trp can be improved by CD-MIPHS. The Bragg diffraction peak of CD-MIPHS redshifted 126 nm when the CD-MIPHS were immersed into a series concentration of L-Trp solution, and visually perceptible color change was clear. Moreover, enantioselective recognition of Trp enantiomers was accomplished by CD-MIPHS instead of PAM-MIPHS. In short, the resultant CD-MIPHS showed rapid response, high selectivity, high sensitivity and specificity towards the imprinted molecules in an aqueous environment.

Introduction

Molecular imprinting technology (MIT) is a well-established and facile technique used to synthesize molecularly imprinted polymers (MIPs) with specific binding nanocavities.^{1,2} Owing to the complementarity in shape and binding sites, the created nanocavities exhibit high selectivity towards the imprinted molecules, such as protein,³ resveratrol,⁴ bisphenol A.⁵ Due to the unique properties of high selectivity and structure predictability, MIPs have widely been applied as the recognition elements in analytical techniques. There are many studies on the highly sensitive and selective hyphenated techniques based on the combination of MIT and other traditional methods, such as chromatography techniques,^{6,7} solid phase extraction (SPE),⁸ electrochemical method⁹ and hydrogel photonic crystals (HPCs)¹⁰⁻¹⁵.

Particularly, Molecularly Imprinted Photonic Hydrogels (MIPHS) based on the combination of MIT and HPCs have attracted considerable interest. MIPHS is characterized by a 3D-ordered interconnected macroporous structure in which numerous recognition nanocavities are distributed in the thin polymer wall.¹⁶ The created nanocavities endow MIPHS with high specificity to analyte. Moreover, the molecular recognition events of MIPHS can be directly transferred into visually perceptible color change due to the shift of photonic band-gap.¹⁷ Furthermore, efficient mass transport and easier accessibility to the active sites can easily be accomplished

through the hierarchical porous structure. Therefore, MIPHS have been widely developed for the detection of a large and diverse set of molecules.¹⁸⁻²⁵

However, the specific recognition of all these MIPHS to target analytes was mainly based on hydrogen bonding interactions between template molecules and functional monomers.^{26,27} Hydrogen bonding interactions could not allow the effective detection of hydrophobic molecules when MIPHS employed in aqueous environments. In order to address this issue, β -cyclodextrin (β -CD)-based polymer had been fabricated due to the host-guest interaction between β -CD and various organic hydrophobic molecules with suitable size.^{28,29} As far as we are aware, little attention had been paid to the use of β -CD for the fabrication of inverse opals of MIPHS. In addition, fabricated MIPHS are deposited on a substrate. It has been demonstrated that the adhesion of the thin film can affect the swelling behavior of thin hydrogel films and thereby their sensing property.³⁰ It can be envisaged that this constraint would vanish for free-standing hydrogel films that were peeled from the substrate.

Herein, novel MIPHS were constructed by copolymerizing acrylamide (AM) with β -CD derivatives. The free-standing film was formed by exfoliation in deionized water directly. L-Tryptophan (L-Trp), the typical representative of organic molecules that can interact with β -CD through supramolecular interactions, was chosen as the model analyte. The recognition properties of MIPHS were demonstrated in detail. The proposed MIPHS can provide higher sensitivity, specificity in comparison with other MIPHS.

Experimental

Materials

The Key Laboratory of Food Colloids and Biotechnology, Ministry of Education, School of Chemical and Material Engineering, Jiangnan University, Wuxi 214122, P. R. China, E-mail: liushirong1@aliyun.com

Electronic Supplementary Information (ESI) available: [details of any supplementary information available should be included here]. See DOI: 10.1039/x0xx00000x

Acrylamide (AM), L-Tryptophan (L-Trp), D-Tryptophan (D-Trp), L-Tyrosine (L-Tyr), L-Phenylalanine (L-Phe), N,N-dimethylformamide (DMF) and maleic anhydride (MAH) were purchased from Sinopharm Chemical Reagent Co., Ltd. (China). 2,2-Diethoxyacetophenone (DEAP) was obtained from TCI (Shanghai) Chemical Industry Development Co., Ltd. N,N'-methylene bisacrylamide (BIS) and β -cyclodextrin (β -CD) were purchased from Aladdin Chemistry Co., Ltd. (China) and β -CD was purified two times by recrystallization from water, and then dried under vacuum at 110 °C for 24 h prior to use. Styrene was purified by distillation under vacuum. All other affiliated chemicals not mentioned here were used without further purification. Glass slides (76.2×24.5×1 mm) for colloidal crystal growth were well-cleaned using acetone, anhydrous ethanol and double-distilled water in an ultrasonic bath in succession.

Synthesis of β -CD based reactive monomer (MAH- β -CD)

In order to integrate β -CD units with the polymer hydrogels, MAH- β -CD carrying five vinyl carboxylic acid groups was easily prepared as elucidated in reference.³¹ Typically, 0.005 mol of β -CD (5.6820 g) was added to 30 mL DMF, and then in which 0.05 mol of MAH (4.9030g) was dissolved. Afterwards, the clear mixture was heated at 80 °C for 10 h under mechanical agitation. The reacted mixture was cooled to room temperature, and then was dropwise added into 30 mL of chloroform. Finally, a yellow precipitate was obtained by washing with large amount of acetone at least three times, and drying in a vacuum oven at 80 °C for 48 h. FT-IR spectra of β -CD and MAH- β -CD were shown in supporting information Fig. S1. And the result of element analysis showed that five primary hydroxyl groups had reacted with MAH.

Preparation of polystyrene (PS) colloidal crystals

The monodispersed PS colloids were synthesized by emulsifier-free emulsion polymerization as described in our previous work.³² Then, corresponding PS colloidal crystal templates were fabricated by vertical deposition method. Briefly, PS colloid particles suspensions with a weight concentration of approximately 1 % were poured into clean containers, then glass slides were inserted vertically into the above solution. Subsequently, the containers were placed in constant temperature humidity chamber. After the solvent was evaporated completely, PS colloidal crystals were deposited on the glass slide.

Preparation of free-standing molecularly imprinted photonic hydrogels (MIPHs)

In this work, two types of MIPHs, called CD-MIPHs or PAM-MIPHs respectively, were fabricated according to whether MAH- β -CD was involved in or not. Prior to fabrication of MIPHs, a homogeneous precursor of MAH- β -CD (0.75 mmol or 0 mmol), AM (25 mmol), BIS (1.5 mmol), DEAP (50 μ L), and L-Trp (0.3 mmol) in 5 mL of phosphate buffer solution (pH 7.4) was

deoxygenated under nitrogen for 10 min. "Sandwich structure" was firstly obtained by covering PS colloidal crystal templates with quartz glass plate of suitable size and immobilizing tightly. Based on this structure the precursors could infiltrate in the interstitial of PS colloidal crystal templates by capillary-attraction-induced force. Polymerization of the filled mixtures was conducted in an ice bath by irradiation at 254 nm for 2 h, and composite opal film was eventually formed on the glass slide. To obtain a free-standing photonic hydrogel, composite opal film was immersed in H₂O. The hydrogel film would detach from the substrate in several minutes. The exfoliated composite opal film was immersed in dimethylbenzene to completely etch the PS colloids, and subsequently incubated in methanol/acetic acid (9/1, v/v) to elute L-Trp molecules. The corresponding non-molecularly imprinted photonic hydrogels (NIPHs) were also prepared under the same preparation conditions but in the absence of L-Trp.

Characterization

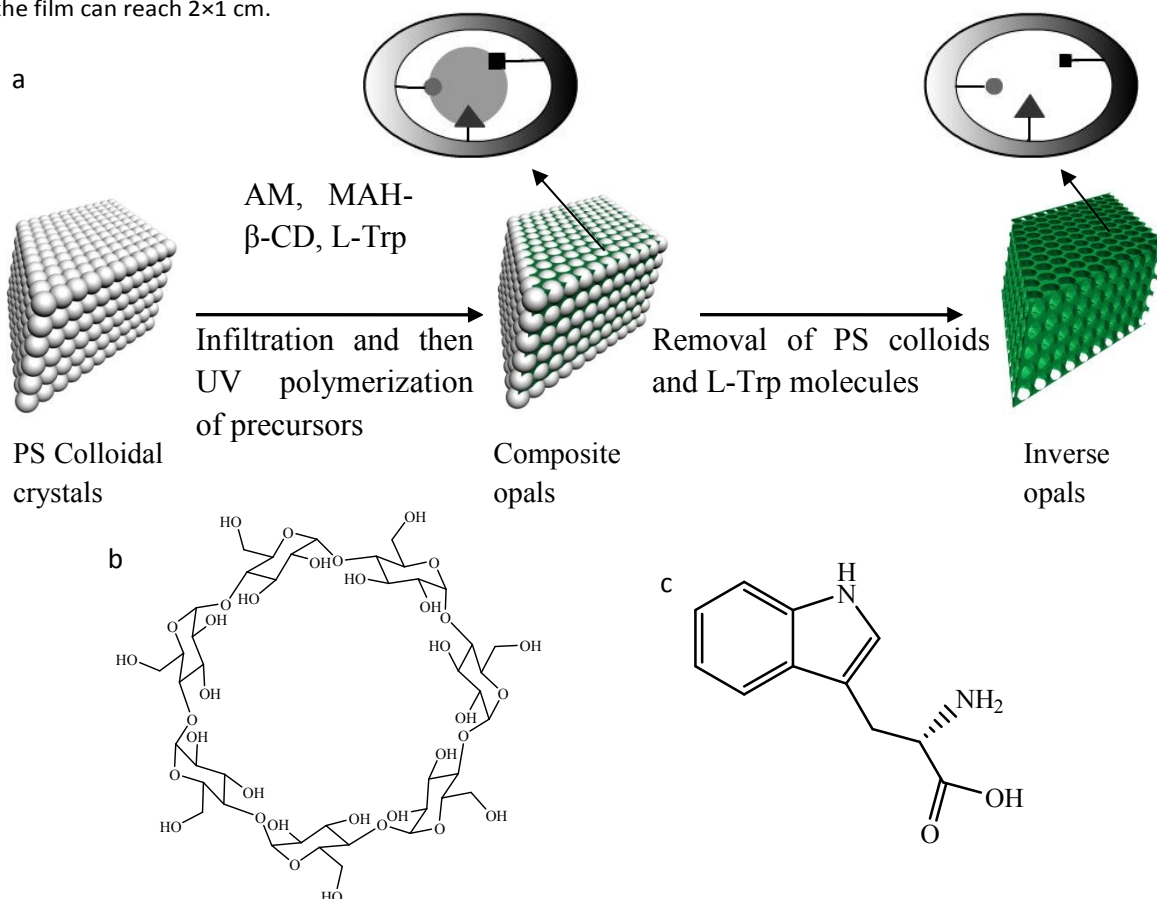
Surface morphologies of PS Colloidal Crystals and inverse opals of MIPHs were characterized by field emission scanning electron microscopy (SEM, Hitachi, S-4800). The Bragg diffraction wavelength of MIPHs that were immersed in the relevant solution of various concentrations was recorded by a miniature fiber optic spectrometer (FLA 4000+, China). The corresponding color changes were photographed using a common digital camera under a daylight lamp. UV spectra of the inclusion complexes of L-Trp and β -CD of different concentrations were measured on a TU-1901 UV-vis spectrophotometer. FT-IR spectra of β -CD and MAH- β -CD were recorded on a Nicolet Nexus 470 spectrometer in the optical range of 400–4000 cm⁻¹ by averaging 32 scans at a resolution of 4 cm⁻¹.

Results and discussion

Fabrication of free-standing L-Tryptophan imprinted photonic hydrogels

Three-step procedure well-established for the construction of MIPHs was shown in Scheme 1, including the preparation of PS colloidal crystals, the infiltration and polymerization of precursors in the interstitial of colloidal crystals, and the removal of the PS template and imprinted L-Trp molecule. It should be underlined that there is a remarkable improvement in the process of infiltration of precursors. While permeating of precursors into the PS interstitials, it was tilted by about 30° against the horizontal, and then precursors was dropped on the bottom edge of "sandwich structure" using a 5 μ L pipette. Spontaneously, mixtures were slowly drawn into the space of the "sandwich structure" by capillary-attraction-induced force. Through polymerization, the polymer film was deposited on the substrate. To make the film easily remove from the substrate, the sequence of soaking in water and immersing into xylene must not be reversed. Only in this case the free-standing MIPHs can be acquired and the largest fabrication

size of the film can reach 2×1 cm.



Scheme 1. (a) Schematic illustration of the procedure for the preparation of inverse opals of MIPHS and molecular structures of (b) β -CD and (c) L-Trp.

Fig. S1 exhibited the typical SEM photos of the adopted colloidal-crystal template and the resultant hydrogel inverse opal film with a thickness of about 100 μ m. Highly ordered PS colloidal crystals had been prepared by vertical deposition of the PS colloids (210 nm) onto a glass substrate (Fig. S1a). After removal of PS colloids and L-Trp molecules, as it can be seen clearly in Fig. S1b, c, 3D highly ordered and interconnected macroporous arrays with a thin polymer wall of approximately 50 nm were obtained successfully. The hierarchical macroporous structure was essential for the easier accessibility to the specific nanocavities after etching PS colloid. Moreover, the photograph of exfoliated film was also given in Fig. S1d, showing the liberation of photonic hydrogels from the substrate successfully.

Recognition property of PAM-MIPHS

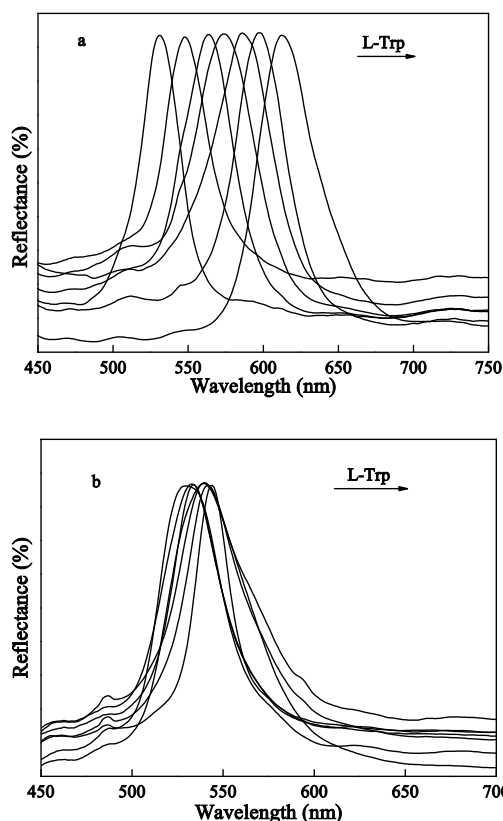


Fig. 1 Optical response of PAM-MIPHS (a) and PAM-NIPHS (b)

upon soaking in L-Trp buffers. (c) Color change of PAM-MIPHS.

Amino acids would show different forms (cation, zwitterion and anion) in solutions with various pH. Minor structural difference of imprinting molecules in the fabrication of the MIPHS may result in different nanocavities in configuration. That would exert effect on the recognition properties of MIPHS. In order to maintain the uniformity of specific binding sites, existing state of L-Trp in precursors needs to be certain. Therefore, the pH of the precursors was constant 7.4 in our work. Furthermore, recognition properties of MIPHS were investigated in the analyte solution with the same pH (7.4). Fig. 1 displayed reflectance spectra of PAM-MIPHS and PAM-NIPHS upon soaking in buffer solutions with the L-Trp concentration at 10^{-10} M, 10^{-9} M, 10^{-8} M, 10^{-7} M, 10^{-6} M, and 10^{-5} M. The Bragg diffraction peak of the PAM-MIPHS soaked in 10^{-5} M L-Trp was already redshifted by 83 nm relative to that of the original blank PAM-MIPHS in phosphate buffer solution, whereas only a slight shift (13 nm) was detected by the PAM-NIPHS. Furthermore, even upon exposure to 10^{-12} M L-Trp buffer solutions, the Bragg diffraction peak of PAM-MIPHS showed about 3 nm shift. Therefore, the detection limit of PAM-MIPHS approached 10^{-12} M.

Bragg diffraction wavelength (λ_{\max}) is determined by the Bragg diffraction law³³⁻³⁵ as

$$\lambda_{\max} = 2(d_{hkl}/m)(D/D_0)(n_{\text{eff}}^2 - \sin^2\theta)^{1/2} \quad (1)$$

where d_{hkl} is the interplanar distance of two neighboring layers along the incident direction, n_{eff} is the effective refractive index, and D/D_0 is the degree of swelling of the gel where D and D_0 denote the equilibrium diameters of the hydrogel at a given condition and in the reference state, respectively. For thin films of MIPHS, the top layers typically correspond to the (111) plane, so that $d_{hkl}=0.8165d$, where d is the diameters of PS colloids. Thus, eq. 1 simplifies to give

$$\lambda_{\max} = 1.633(d/m)(D/D_0)(n_{\text{eff}}^2 - \sin^2\theta)^{1/2} \quad (2)$$

For specific MIPHS, $d=210$ nm, $m=1$, $\theta=0^\circ$.

The effective refractive index (n_{eff}) can be expressed as

$$n_{\text{eff}} = [n_w^2(1-f) + n_m^2f]^{1/2} \quad (3)$$

in which n_w and n_m are the average refractive indices of the PAM walls (1.48) and medium H₂O (1.33), respectively. $f=0.74$ (fcc structure) is the filling factor of PS colloids. So the factor that affects λ_{\max} is D/D_0 .

The change of D/D_0 was essentially attributed to the specific adsorption of L-Trp molecules to imprinting nanocavities. After adsorbing L-Trp molecules, concentration gradients of L-Trp between hydrogel and hydrous solution could be formed, and the more L-Trp molecules adsorbed, the greater concentration gradients formed. Then, water penetrated into hydrogel phase, resulting in the swelling of inverse opal. Therefore, the Bragg

diffraction peak of PAM-MIPHS redshifted marked with the increase of L-Trp concentration. There are not specific nanocavities distributed in PAM-NIPHS. The slight redshift of the peak was due to the nonspecific adsorption of hydrogel to L-Trp molecules.

Recognition property of CD-MIPHS

The prerequisite for creating specific binding nanocavities in the polymer matrix lies in the formation of stable complex between monomers and template molecules L-Trp through strong molecular interactions during the molecular imprinting process. The stronger molecular interactions are, the more specific binding nanocavities would be acquired. Considering strong supramolecular interactions between β -CD and hydrophobic molecules, an appropriate amount of β -CD based reactive monomer (MAH- β -CD) was introduced to enhance the bonding in the pre-polymerization complex. Fig. 2a displayed the sensing behavior of the resultant CD-MIPHS with a series concentration of L-Trp (10^{-10} M, 10^{-9} M, 10^{-8} M, 10^{-7} M, 10^{-6} M, and 10^{-5} M). In contrast with PAM-MIPHS (Fig. 1a), CD-MIPHS showed a higher sensitivity at the same L-Trp concentration. L-Trp at a concentration of 10^{-5} M induced a Bragg diffraction redshift of 126 nm from 525 nm to 651 nm. As shown in Fig. 2b, CD-MIPHS exhibited obvious color change. Encouraged by these promising results, the effect of the content of MAH- β -CD, AM and BIS on imprinting effect were investigated (Fig. S3). The molar ratio between the functional monomers (MAH- β -CD and AM) and cross-linker (BIS) should be balanced.

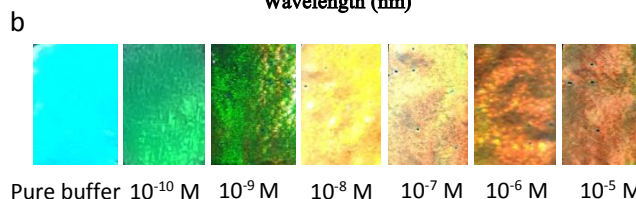
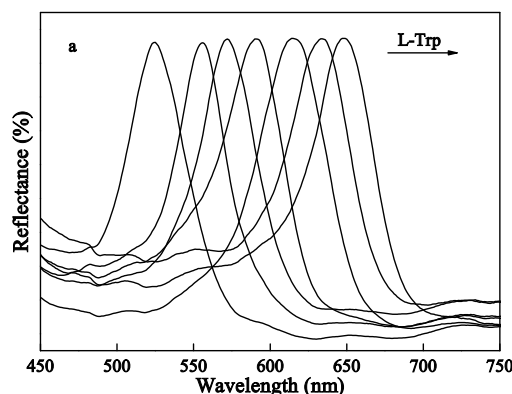


Fig. 2 (a) Optical response of CD-MIPHS upon soaking in L-Trp buffers. (b) Color change of CD-MIPHS induced by the rebinding of L-Trp at different concentrations.

During the molecular imprinting process, the formation of MAH- β -CD-L-Trp inclusion complexes would greatly be of importance. That is beneficial for the construction of specific binding sites. The increase of Bragg diffraction peak shift may

be attributed to the increase of effective binding nanocavities and the strong supramolecular interaction between binding sites and L-Trp molecules. The inclusion interaction could be analyzed by the UV spectra of the inclusion complexes. Fig. 3a presented absorbance change of L-Trp upon addition of different concentrations of MAH- β -CD to 0.05 mM L-Trp solution. The absorbance intensity of the free L-Trp increased gradually with increasing concentration of MAH- β -CD. That may be due to more L-Trp formed inclusion complex with MAH- β -CD, resulting in the diminishment of free L-Trp in solution. According to the Benesi-Hildebrand method,³⁶ the stoichiometry ratio and stability constant can be determined by the following equation

$$\frac{1}{A - A_0} = \frac{1}{\Delta \xi \times [C_{Trp}]_0} + \frac{1}{\Delta \xi \times [C_{Trp}]_0 \times k \times [MAH - \beta - CD]^n_0}$$

where A and A_0 are the absorbance of Trp at each MAH- β -CD concentration and in the absence of MAH- β -CD, respectively. k is the stability constant for inclusion complexation. $[MAH - \beta - CD]_0$ and $[C_{Trp}]_0$ are the original concentrations of MAH- β -CD and L-Trp molecules, respectively, and n represents the stoichiometry ratio of the inclusion complexes. $\Delta \xi$ is the differential molar extinction coefficient of L-Trp in the absence and presence of β -CD. Kong et al.⁹ have reported the stoichiometry ratio and stability constant for the combination of β -CD and the Trp isomers. In theory the stoichiometry ratio would not be changed, and we assumed that n kept a value of 1 in this work, and a straight line is obtained (Fig. 3b), indicating formation of the 1:1 complexes between MAH- β -CD and the L-Trp. The interaction constant k could be calculated to be 233.0 M⁻¹, which was slightly less than the value (254.6 M⁻¹) of inclusion constant between β -CD and the L-Trp. The strong supramolecular interaction allowed the β -CD based reactive monomer competent during the molecular imprinting process.

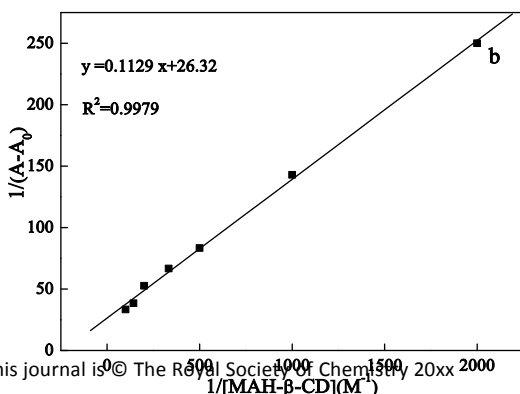
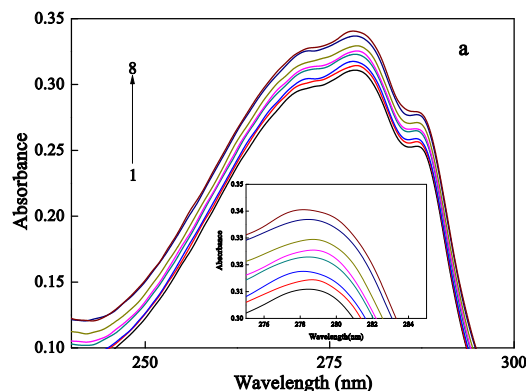


Fig. 3 (a) UV spectra of MAH- β -CD-L-Trp inclusion complexes dependent on various concentrations of MAH- β -CD: (1) 0 mM, (2) 0.5 mM, (3) 1 mM, (4) 2 mM, (5) 3 mM, (6) 5 mM, (7) 7 mM, and (8) 10 mM. (b) Benesi-Hildebrand plot for the inclusion complexes.

Enantioselective recognition of L-Trp and D-Trp

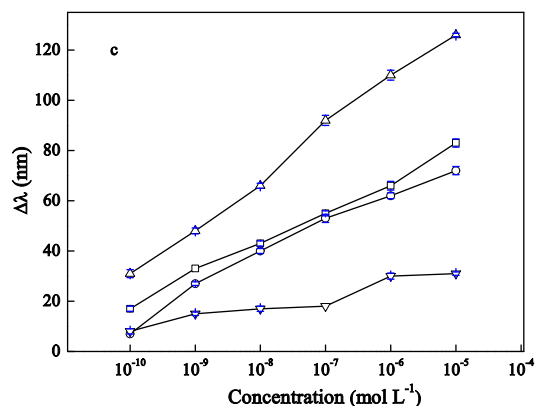
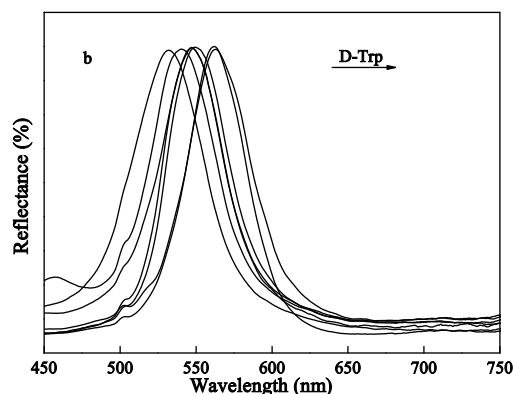
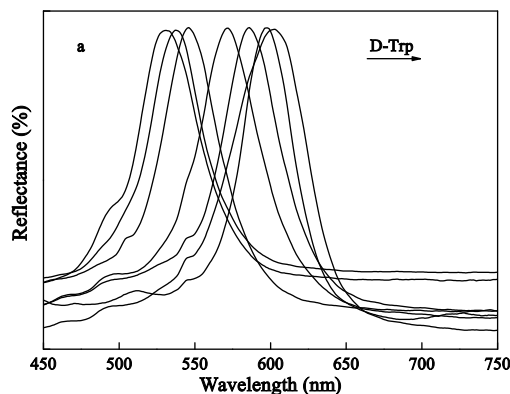


Fig. 4 Optical response of (a) PAM-MIPHs and (b) CD-MIPHs upon soaking in D-Trp buffers. (c) Plots of Bragg diffraction peak shifts of PAM-MIPHs to L-Trp (\square), D-Trp (\circ) and CD-MIPHs to L-Trp (\triangle), D-Trp (∇).

Fig. 4 showed the sensing behavior of the resultant PAM-MIPs and CD-MIPs with a series concentration of D-Trp. The response of PAM-MIPs to D-Trp (Fig. 4a) was similar to that of PAM-MIPs to L-Trp (Fig. 1a). That indicated that PAM-MIPs could not distinguish stereoisomer of Trp. The shift of Bragg diffraction peak of CD-MIPs with a series concentration

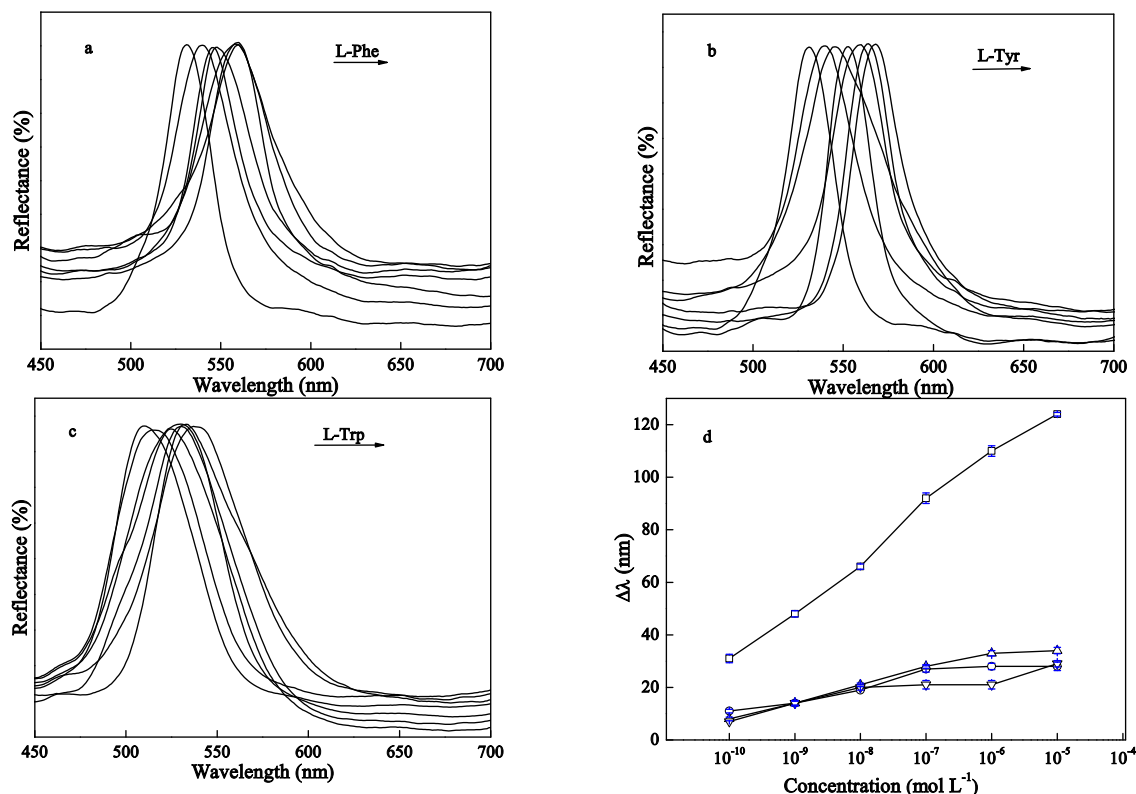


Fig.5 Optical response of CD-MIPs upon soaking in (a) L-Phe buffers and (b) L-Tyr buffers, respectively. (c) Optical response of CD-NIPs upon soaking in L-Trp buffers. (d) Plots of Bragg diffraction peak shifts for CD-MIPs to L-Trp (□), L-Phe (○), L-Tyr (△) and CD-NIPs to L-Trp (▽).

of D-Trp was relatively slight compared with the result (126 nm) of Fig. 2a, indicating that CD-MIPs possessed higher stereoselectivity. It can be envisaged that the stereoselectivity of CD-MIPs are tightly related to the incorporation of β -CD. Specific binding nanocavities with particular shape, size and binding sites were involved in the PAM-MIPs and CD-MIPs. But owing to the tiny configuration difference between L-Trp and D-Trp, nanocavities of PAM-MIPs were not competent for the enantioselective recognition of L-Trp and D-Trp. Assisted by the stereoselective discrimination of Trp enantiomers by β -CD, fabricated CD-MIPs can easily differentiate Trp enantiomers. However, due to the presence of nonspecific binding sites during the molecular imprinting process, CD-MIPs would adsorb a certain amount of nonimprinted molecules, resulting in the minor redshift (37 nm) of Bragg diffraction peak. Although nonspecific binding of CD-MIPs led to the redshift of Bragg diffraction peak, the effect of molecular imprinting still dominated.

Selectivity of CD-MIPs

According to above results, fabricated CD-MIPs exhibited the

better sensitivity and stereoselectivity. Besides, selectivity of CD-MIPs towards L-Phe and L-Tyr was also investigated. The corresponding reflectance spectra were revealed in Fig. 5. Compared with the result of CD-MIPs to L-Trp, slight optical redshifts of CD-MIPs induced by L-Phe and L-Tyr took place under the same measurement conditions. The reason is believed to be that imprinted nanocavities with the fixed shape, size and interaction sites can bind much more L-Trp molecules than L-Tyr and L-Phe. These results indicated that fabricated CD-MIPs can efficiently discriminate between template and the analog owing to the cooperative effect of shape, size, and interaction sites of the imprinted nanocavities. To further elucidate imprinting effect of CD-MIPs, reflectance spectra of CD-NIPs upon exposure to L-Trp buffers were shown in Fig. 5c. Probably due to the nonspecific adsorption, only a slight fluctuation in the Bragg peak was observed in contrast with the sensing behavior of CD-MIPs. In summary, CD-MIPs had the superior ability to selective recognize template molecules.

Response speed and recoverability of CD-MIPs

Although the thickness (100 μm) of our free-standing CD-

MIPHS was thicker than reported obviously ($2\ \mu\text{m}$)^{37,38}, fast response could still be accomplished (Fig. 6a). It only needed 30 s to nearly reach its highest Bragg diffraction peak when CD-MIPHS were immersed into the $10^{-5}\ \text{M}$ L-Trp solution. The 3D interconnected macroporous structure was favorable for molecular diffusion, and the recognition sites that are situated at the surface or in proximity to the surfaces of the ultrathin polymer wall, were easily accessible. On the other hand, the swelling behavior of exfoliated film was no longer restricted by the substrates. Therefore, free-standing CD-MIPHS exhibited rapid response speed all the same. Moreover, the responded CD-MIPHS can be easily recovered by using methanol/acetic acid to remove rebinding molecules. Fig. 6b showed the recoverability of free-standing CD-MIPHS over five cycles between pure buffer and $10^{-5}\ \text{M}$ L-Trp solution. This indicated that CD-MIPHS have good recoverability, which makes it useful for practical applications. Moreover, the free-standing film can remain intact and maintain excellent recognition property even stored for half a year. Compared to other strategies^{39,40} concerning the recognition of Trp, CD-MIPHS overcome the shortcomings such as high cost and time consumption. However, although the sensitivity and selectivity of CD-MIPHS can retain high levels, quantitative detection of MIPHS still needs further research.

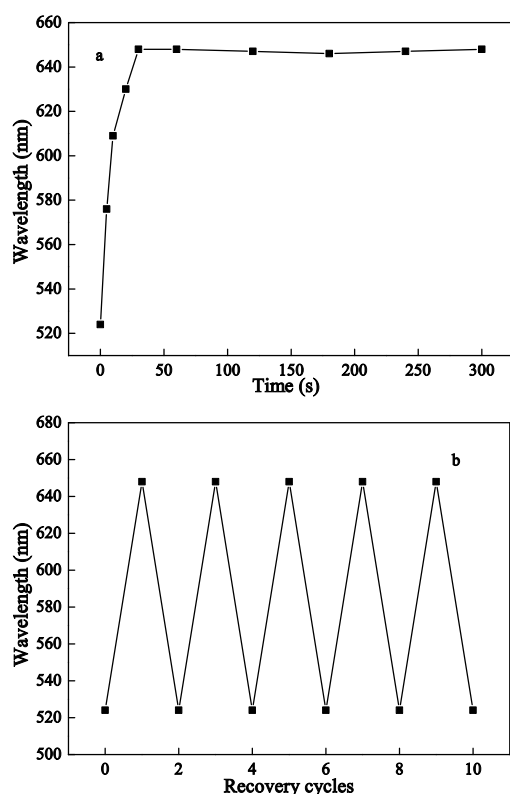


Fig. 6 Kinetic response (a) and recoverability (b) of free-standing CD-MIPHS.

Conclusions

In summary, inverse opals of molecularly imprinted photonic hydrogels (CD-MIPHS) containing β -CD were successfully developed. The CD-MIPHS demonstrated higher sensitivity and better chiral recognition for Trp enantiomers. And CD-MIPHS also exhibited highly selectivity to analogous molecules. In addition, the thin film can be exfoliated from the substrate to produce an intact free-standing CD-MIPHS film. The peeled free-standing inverse opal film might provide great convenience for the application in the real-world environments. This study not only provided a method for the detection of L-Trp, but opened an avenue for the detection of many other molecules in aqueous environments. However, further investigations still needed to minimize non-specific adsorption.

Acknowledgements

This study was supported by the National Natural Science Foundation of China (No. 51173072), the Fundamental Research Funds for the Central Universities (JUSRP51408B), and MOE & SAFEA for the 111 Project (B13025).

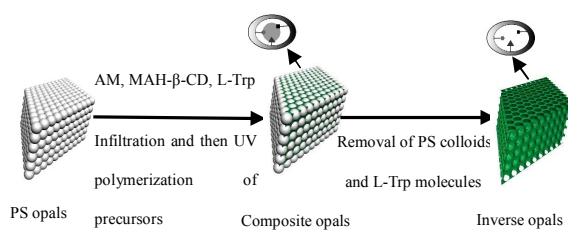
References

- Haupt and K. Mosbach, *Chemical reviews*, 2000, **100**, 2495-2504.
- X. Chen, S. F. Xu and J. H. Li, *Chemical Society Review*, 2011, **40**, 2922-2942.
- Taguchi, H. Sunayama, E. Takano, Y. Kitayama and T. Takeuchi, *Analyst*, 2015, **140**, 1448-1452.
- F. Chen, X. Y. Xie and Y. P. Shi, *Journal of Chromatography A*, 2013, **1300**, 112-118.
- Inoue, T. Ooya and T. Toshifumi, *Microchim Acta*, 2013, **180**, 1387-1392.
- Shaikh, N. Memon, H. Khan, M. I. Bhangar and S. M. Nizamani, *Journal of Chromatography A*, 2012, **1247**, 125-133.
- M. Moein, A. El-Beqqali, M. Javanbakht, M. Karimi, B. Akbari-adergani and M. Abdel-Rehim, *Journal of Chromatography A*, 2014, **1372**, 55-62.
- Bitar, P. Cayot and E. Bou-Maroun, *Analytical Methods*, 2014, **6**, 6467-6472.
- X. Tao, J. Y. Dai, Y. Kong and Y. Sha, *Analytical chemistry*, 2014, **86**, 2633-2639.
- A. Asher, J. Holtz, L. Liu and Z. J. Wu, *Journal of the American Chemical Society*, 1994, **116**, 4997-4998.
- T. Tian, J. X. Wang, Y. M. Zheng, Y. L. Song, L. Jiang and D. B. Zhu, *Journal of Materials Chemistry*, 2008, **18**, 1116-1122.
- Hu, X. W. Zhao, Y. J. Zhao, J. Li, W. Y. Xu, Z. Y. Wen, M. Xu and Z. Z. Gu, *Journal of Materials Chemistry*, 2009, **19**, 5730-5736.
- L. Jiang, Y. H. Zhu, C. Chen, J. H. Shen, H. Bao, L. M. Peng, X. L. Yang and C. Z. Li, *New Journal of Chemistry*, 2012, **36**, 1051-1056.
- Y. Cai, J. T. Zhang, F. Xue, Z. M. Hong, D. Punihaole and S. A. Asher, *Analytical chemistry*, 2014, **86**, 4840-4847.
- T. Zhang, Z. Y. Cai, D. H. Kwak, X. Y. Liu and S. A. Asher, *Analytical chemistry*, 2014, **86**, 9036-9041.
- B. Hu, Q. An, G. T. Li, S. Y. Tao and B. Liu, *Angewandte Chemie-International Edition*, 2006, **45**, 8145-8148.
- Nojima, G. Kaneda and K. Aizawa, *Journal of Applied Physics*, 2013, **113**, 123105.

ARTICLE

Journal Name

- 18F. Liu, S. Y. Huang, F. Xue, Y. F. Wang, Z. H. Meng and M. Xue, *Biosensors & bioelectronics*, 2012, **32**, 273-277.
- 19D. Xu, W. Zhu, Y. Jiang, X. S. Li, W. N. Li, J. C. Cui, J. X. Yin and G. T. Li, *Journal of Materials Chemistry*, 2012, **22**, 16572-16581.
- 20L. Q. Wang, F. Y. Lin and L. P. Yu, *Analyst*, 2012, **137**, 3502-3509.
- 21F. Xue, Z. Meng, Y. Wang, S. Huang, Q. Wang, W. Lu and M. Xue, *Analytical Methods*, 2014, **6**, 831-837.
- 22N. Sai, B. Ning, G. Huang, Y. Wu, Z. Zhou, Y. Peng, J. Bai, G. Yu and Z. Gao, *Analyst*, 2013, **138**, 2720-2728.
- 23Y. L. Zhang, Z. Pan, Y. X. Yuan, Z. M. Sun, J. K. Ma, G. B. Huang, F. B. Xing and J. P. Gao, *Physical Chemistry Chemical Physics*, 2013, **15**, 17250-17256.
- 24J. Li, Z. Zhang, S. Xu, L. Chen, N. Zhou, H. Xiong and H. Peng, *Journal of Materials Chemistry*, 2011, **21**, 19267.
- 25H. Peng, S. Wang, Z. Zhang, H. Xiong, J. Li, L. Chen and Y. Li, *Journal of agricultural and food chemistry*, 2012, **60**, 1921-1928.
- 26Y. X. Zhang, P. Y. Zhao and L. P. Yu, *Sensors and Actuators B: Chemical*, 2013, **181**, 850-857.
- 27Y. Yuan, Z. Li, Y. Liu, J. Gao, Z. Pan and Y. Liu, *Chemistry-A European Journal*, 2012, **18**, 303-309.
- 28X. Y. Liu, H. X. Fang and L. P. Yu, *Talanta*, 2013, **116**, 283-289.
- 29L. Qin, X. W. He, W. Y. Li and Y. K. Zhang, *Journal of Chromatography A*, 2008, **1187**, 94-102.
- 30N. Griffete, H. Frederich, A. Maitre, S. Ravaine, M. M. Chehimi and C. Mangeney, *Langmuir*, 2012, **28**, 1005-1012.
- 31Y. Y. Liu and X. D. Fan, *Polymer*, 2002, **43**, 4997-5003.
- 32H. Liu, D. Shi, F. Duan, Z. Yang, M. Chen and S. Liu, *Material Letter*, 2015, **150**, 5-8.
- 33J. Y. Wang, Y. Cao, Y. Feng, F. Yin and J. P. Gao, *Advanced materials*, 2007, **19**, 3865-3871.
- 34G. I. N. Waterhouse and M. R. Waterland, *Polyhedron*, 2007, **26**, 356-368.
- 35A. Stein, B. E. Wilson and S. G. Rudisill, *Chemical Society reviews*, 2013, **42**, 2763-2803.
- 36H. Benesi and J. Hildebrand, *Journal of the American Chemical Society*, 1949, **71**, 2703-2707.
- 37Z. Wu, C. A. Tao, C. X. Lin, D. Z. Shen and G. T. Li, *Chemistry-A European Journal*, 2008, **14**, 11358-11368.
- 38L. Meng, P. Meng, Q. Zhang and Y. Wang, *Analytica chimica acta*, 2013, **771**, 86-94.
- 39Y. Kong, J. X. Wei, W. C. Wang and Z. D. Chen, *Electrochim Acta*, 2011, **56**, 4770-4774.
- 40S. Ghosh, T. H. Fang, M. S. Uddin and K. Hidajat, *Colloids and Surfaces B-Biointerfaces*, 2013, **105**, 267-277.



Molecularly imprinted photonic hydrogels fabricated by colloidal crystal template method have been exfoliated from substrate to get a free-standing film.

1
2
3
4
5
6
7
8
9
10
11
12
13
14
15
16
17
18
19
20
21
22
23
24
25
26
27
28
29
30
31
32
33
34
35
36
37
38
39
40
41
42
43
44
45
46
47
48
49
50
51
52
53
54
55
56
57
58
59
60